Effects of Axial Load and Tensile Strength on Reinforced UHPC Plastic Hinge Length

Joseph A. Almeida – Graduate Research Assistant, New Jersey Institute of Technology, Department of Civil and Environmental Engineering, Newark, NJ, Email: ja558@njit.edu

Matthew J. Bandelt, Ph.D. P.E. (corresponding author) – Associate Professor and Associate Dean for Research and Graduate Studies, New Jersey Institute of Technology, Department of Civil and Environmental Engineering, Newark, NJ, Email: bandelt@njit.edu

Abstract:

Researchers have explored the high energy absorption capacity and strength of UHPC materials to improve the seismic performance of structural components. Experimental results in the literature of reinforced UHPC members have indicated superior damage tolerance, higher strength and deformation capacities, and lower potential for collapse across a range of structural components. Investigations into the underlying failure mechanisms have highlighted the significance of the synergy between material tensile strength and reinforcement properties on member flexure response. Although research into the seismic application of reinforced UHPC continues to expand, relatively little is known about the effects of varying axial load on the plastic hinge response of beam-column elements across a range of UHPC tensile properties and reinforcement levels. Therefore, in this study, the effects of varying tensile properties on beam-column elements through numerical simulations across a range of axial load ratios were investigated. Two dimensional numerical models accounting for material nonlinearities (e.g., bond-slip, UHPC tensile strength and strain capacity) were used to capture component responses. Trends in the moment-drift responses and plastic hinge lengths have highlighted the diminishing returns of using higher fiber volume percentages (2%) as higher axial loads tend to relieve tensile demands. Additionally, existing plastic hinge length expressions for RC components were found to over-predict hinge length consistently while those developed for HPFRCC components accurately predict plastic hinge lengths at low axial load levels.

Keywords: Ultra High-Performance Concrete, column, simulation, plastic hinge length, finite element analysis

1. Introduction

Ultra-High-Performance Concrete (UHPC) has increasingly been implemented in engineering projects ranging in a variety of applications such as expansion joints, component overlays, and precast decks (Russell & Graybeal, 2013). Realizing its enhanced performance, recent research endeavors have focused on the deployment of UHPC for seismic applications in columns. Such testing of components under quasi-static cyclic loading conditions has demonstrated significant improvements in strength, deformation, and energy absorption capacity when compared to traditional reinforced concrete (Aboukifa & Moustafa, 2021). Further, investigations into the

structural level behavior of ductile cementitious materials, similar to UHPC, have indicated changes in potential for collapse (Tariq et al., 2021) and better construction economy (Gencturk, 2013), with the caveat that component-level designs directly consider their improved mechanical properties (Gencturk, 2013; Tariq et al., 2021).

To this end, the deployment of UHPC for seismic applications is promising, but a greater understanding of how UHPC's mechanical properties affect column behavior is needed. Moreover, critical engineering tools used for evaluating structural level performance must be developed considering the unique properties of UHPC. Therefore, the study herein investigates the effects of varying UHPC tensile properties, reinforcement ratios, and applied axial load levels on plastic hinge mechanisms and responses of columns through a series of numerical simulations. The results are discussed and recommendations for future UHPC research are made.

2. Background

UHPC is a class of high-performance fiber-reinforced cementitious composite (HPFRCC) that exhibits both strain and deflection hardening behavior when subjected to tension (Wille et al., 2014). Its unique mechanical properties can be attributed to the cementitious matrix packing density as well as the inclusion of short discontinuous steel fibers. Over the past two decades, numerous studies have developed UHPC mixes across a range of material strengths (Wille & Boisvert-Cotulio, 2013). UHPC's compressive and tensile strengths have been reported to vary from 120-200 MPa (17.4-29 ksi) and 5-14 MPa (0.73-2 ksi) respectively. Although many UHPC mixture designs have been proposed, many commercially available UHPC mixes use proprietary blends with discrete levels of mechanical performance. Nonetheless, engineers do have control over the addition of steel fibers which has been shown to play an influential role in UHPC tensile strength, component response, and cost (Shao & Billington, 2022; Wille et al., 2014; Wille & Boisvert-Cotulio, 2013).

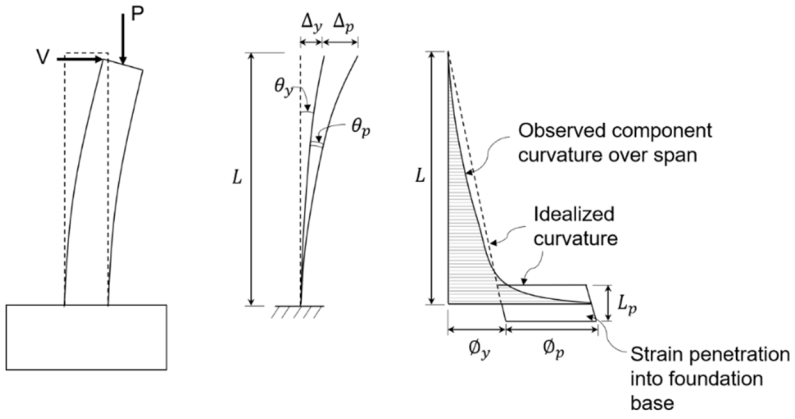

Figure 1. Equivalent plastic hinge conceptualization.

The congruent development of performance-based displacement design has made the use of nonlinear analysis more pervasive in engineering practice. Now more than ever, engineers are faced with the challenge of accurately capturing the hysteretic behavior of structures in order to quantify structural performance. To accomplish this task, engineers often employ computationally

efficient lumped plasticity models which simulate the nonlinear behavior associated with concrete crushing, bond-slip, and rebar buckling over a predefined length typically located in regions where plasticity is concentrated (Applied Technology Council, 2017). As illustrated in Figure 1, the predefined length, often termed the plastic hinge length or equivalent plastic hinge length is a fictitious length over which the plastic curvature of sections is assumed to be constant (Paulay & Priestley, 1992). By assuming a linear strain distribution (i.e., Euler-Bernoulli Beam Theory) and employing the concepts for plastic hinge length (see Pokhrel & Bandelt, 2019 for full review), the ultimate displacement capacity of members can be calculated as shown in Equation 1 where θ_y is defined as the rotation of the component at first yield, θ_p is the plastic rotation, and θ_u is the rotation at collapse (e.g., tension reinforcement fracture or a 20% reduction of load carrying capacity). Moreover, $\emptyset_y$ is the section curvature at first yield, $\emptyset_u$ is the section curvature at collapse, and L is the component span length. By rearranging Equation 1, Equation 2 can be derived such that the plastic hinge length, L_p, of any structural component can be calculated.

$$\theta_u = \theta_y + \theta_p = \frac{1}{2}\emptyset_y L + (\emptyset_u - \emptyset_y)L_p \quad (1)$$

$$L_p = \frac{\theta_u - \theta_y}{\emptyset_u - \emptyset_y} \quad (2)$$

While Equation 2 allows for the direct calculation of the equivalent plastic hinge length of a component, member rotations are typically not known in advance. Consequently, many studies have proposed plastic hinge length expressions so that practicing engineers can readily analyze components with typical design parameters (Paulay & Priestley, 1992; Pokhrel & Bandelt, 2019).

3. Numerical Modeling

Recent developments in finite element modeling have enabled researchers to accurately capture experimentally observed component responses (Bandelt & Billington, 2018; Pokhrel & Bandelt, 2019; Shao et al., 2021). Building off these works, a total of 12 two-dimensional numerical models of a representative experimental cantilever column were simulated using a commercially available finite element software, DIANA FEA 10.5. To investigate the effects of axial load, UHPC tensile properties, and level of reinforcement, a test matrix of $3 \times 2 \times 2 = 12$ was employed. Axial load ratios of 5%, 15%, and 25% were selected to represent levels of low, medium, and high axial load respectively. Columns were symmetrically reinforced either with 0.70% or 1.25% mild tensile reinforcement steel (total of 1.4% and 2.5%) which is representative of typical column reinforcement ranges. Lastly, changes in fiber volume percentages from 1% to 2% were modeled through appropriate changes to the UHPC constitutive tension model that will be discussed in the following sections.

Geometry, Materials, and Analysis

Figure 2a. presents the column geometry, boundary conditions, and loading case of the simulations. The column dimensions were 130 mm×180 mm×1080 mm ($5\ in \times 7\ in \times 42.5\ in$) corresponding

to a column aspect ratio of 6. The foundation beam dimensions were 130 mm×800 mm×380 mm ($5\ in \times 31.5\ in \times 15\ in$).

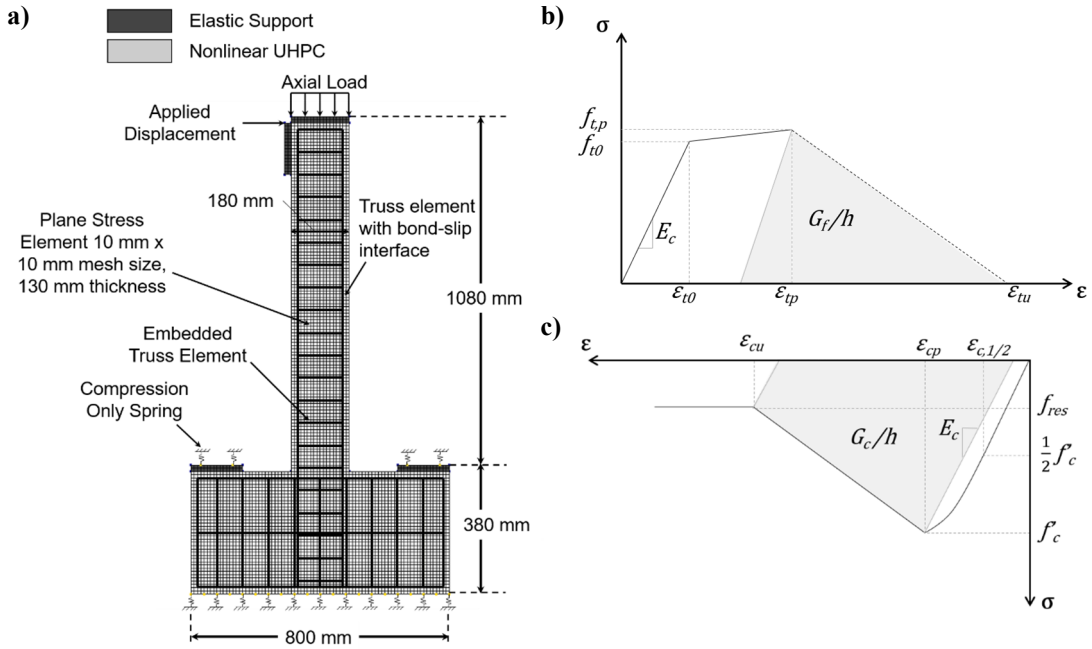

Figure 2. (a) Finite element model setup, (b) UHPC tensile stress-strain envelope adapted from (Shao et al., 2021), and (c) UHPC compressive stress-strain envelope adapted from (Shao et al., 2021).

Symmetrical longitudinal reinforcement corresponding to 0.70% and 1.25% (each side) was provided. To prevent localized damage to the component, linear elastic steel plates were modeled at the load application and column anchorage points. 10 mm×10 mm plane-stress quadrilateral elements with a 3×3 Gaussian integration scheme were used to model the column, foundation beam, and loading plates. Hoop and foundation beam reinforcements were modeled as embedded truss elements with a perfect bond to the UHPC. Longitudinal reinforcements were modeled as a bond-slip reinforcement which integrates a truss element and bond-slip interface.

For this study, the tension failure envelope was modeled as an idealized trilinear response shown in figure 2b. Experimental UHPC tensile properties reported by Alkaysi and Shao for 1% and 2% fiber reinforcement respectively were implemented (Alkaysi & El-Tawil, 2016; Shao & Billington, 2022). Although the derivation of material tensile properties from direct tension tests has been a point of debate, in an attempt to keep all derived material properties consistent, tensile fracture energies were calculated based on the direct tension stress-strain model developed by Wille (Wille et al., 2014).

A UHPC compression model developed by Shao (Shao et al., 2021) was adopted and is shown in Figure 2c. To capture the energy release associated with the gradual crushing of UHPC, the linear softening branch was normalized by the fracture energy and element size. The confining effects of varying fiber reinforcement have been found to affect the post-peak ductility of UHPC – and thus the compressive fracture energy – but due to limited available data on fiber reinforced UHPC below 2%, a constant compressive fracture energy across all simulations was used. In

addition, a residual compressive strength of 20% was selected based on reported experimental results (Naeimi & Moustafa, 2021). Table 1 summarizes the assumed material properties used.

Table 1. Material properties assumed for numerical simulation.

	Notation	Unit	V_f = 2%	V_f = 1%
Tensile strength	f_t	[MPa]	10.5	7.2
Strain at the onset of tensile softening	ε_{tp}	[mm/mm]	0.002	0.0018
Tensile fracture energy	G_f	[N/mm]	20	11.6
Modulus of Elasticity	E_c	[MPa]	50161	50436
Compression strength	f'_c	[MPa]	185.8	187.8
Compression fracture energy	G_c	[N/mm]	180	180
Max bond stress	$\tau_{max,\ \rho=0.70\%}$	[MPa]	32.63	30.25
Max bond stress	$\tau_{max,\ \rho=1.25\%}$	[MPa]	26.38	24.27

To capture the strain hardening effects and bond-slip behavior of the longitudinal reinforcement, a Von Mises plasticity model with a bond-slip law developed by Shao and Ostertag was implemented (Shao & Ostertag, 2022). The maximum bond stress for 1% fiber reinforced UHPC was reduced by 8% based on experimental observations.

A Newton-Raphson iterative method and line search algorithm were used to solve for equilibrium. Convergence of the iterative step was determined when the energy norm of 0.1%, displacement norm of 1%, and force norm of 1% were met. A distributed axial load at the top of the column was applied in a stepwise manner followed by the prescribed lateral deformation of 0.25 mm (0.01 in).

4. Results and Discussion

Figure 3 presents the moment versus drift response of all 12 simulated cantilever columns. Note that at low axial loads (i.e., 5%), the main mode of failure is fracture of the tension reinforcement. This failure mode is in agreement with that observed in experimentally tested UHPC columns of similar axial load levels (Aboukifa & Moustafa, 2021). As the axial load increases to 15%, a shift from tension to compression failure is observed. Moreover, increases in axial load ratio from 5-

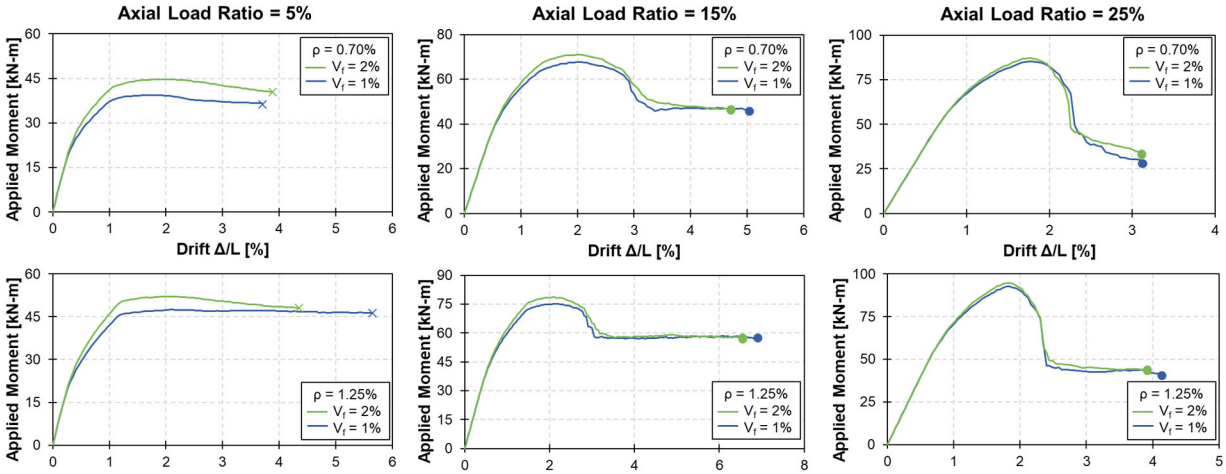

Figure 3. Moment versus drift response of simulated cantilever column. × indicates the fracture of the tension reinforcement, and ● indicates the defined compression limit of the compression reinforcement. In this study, tensile fracture and the compression limit is defined when a reinforcement strain of 0.18 mm/mm is reached.

15% and 15-25% are marked by a sudden loss of load carrying capacity and a decrease in residual strength.

Comparing the moment versus drift responses of 1 and 2% fiber reinforcement reveals diminishing strength capacity benefits associated with 2% fiber reinforcement due to the relief of tensile strains from the applied axial load. In addition, columns with higher UHPC tensile strengths tended to fail at lower drifts due to higher bond strengths and earlier onset of strain hardening (Moreno et al., 2014).

Figure 4 presents the plastic hinge length normalized to the height of the column cross-section as a function of varying UHPC tensile strength, steel reinforcement, and axial load level. Trends in Figure 4a. indicate that plastic hinge length almost doubles from 5% to 15% axial load ratio followed by a plateau. UHPC tensile strength was found to have minimal impact on the plastic hinge length in contrast to moderate increases observed in higher reinforcement ratios. Reviewing of available plastic hinge length expressions of reinforced concrete columns reveals that axial load level is not a typical function of plastic hinge length despite reports of plastic hinge length increasing with axial load level (Bae & Bayrak, 2008). However, reinforcement properties typically affect plastic hinge length due to the additional rotation provided by bond-slip phenomena. Results from a recent study on HPFRCC beam plastic hinge lengths have highlighted the interrelationship between reinforcement ratios and HPFRCC tensile properties on bond-slip phenomena. Therefore, while the UHPC tensile properties in this study were not observed to impact plastic hinge length directly, its effect on plastic hinge length through interdependency with the reinforcement properties cannot be ruled out.

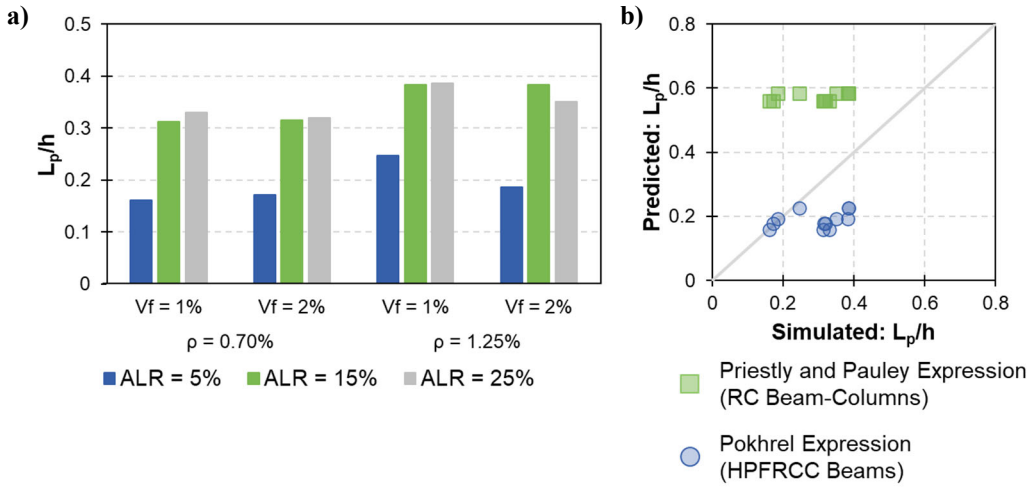

Figure 4. (a) Effect of varying fiber reinforcement, steel reinforcement, and axial load level on normalized plastic hinge length, and (b) comparison of simulated and predicted normalized plastic hinge length.

A comparison of predicted plastic hinge lengths to observed values is presented in Figure 4b. It can be observed that Pauley and Priestly expression (recommended by the FHWA for seismic design and analysis of reinforced concrete bridges) consistently over predicts plastic hinge length values by approximately two times compared to the observed numerical values. These differences can be attributed to the following: i) the original expression was developed for reinforced concrete components which do not consider the tensile properties of the cementitious matrix and, ii) it does

not account for plastic hinge length dependencies on axial load. On the other hand, the plastic hinge length expression developed by Pokhrel and Bandelt (Pokhrel & Bandelt, 2019) for HPFRCC beams accurately captures the plastic hinge length of columns at low axial loads but diverges with increasing axial load levels thus under predicting plastic hinge lengths.

5. Conclusions

In conclusion, the effects of UHPC tensile properties, reinforcement ratios, and axial load levels were explored in this study. Based on the observed trends in the moment versus drift responses and plastic hinge lengths, the response of members with 1% and 2% fiber reinforcement were similar as axial load increased. While this study shows minimal effects of UHPC tensile properties on the column response at medium to high axial loads, future research efforts should explore the relationship between steel reinforcement, steel hardening strength, and UHPC tensile strength in regards to damage levels, delaying reinforcement buckling, and changes in failure paths caused by spalling. In addition, continued efforts should be made in the following areas: i) report complete material properties at lower fiber reinforcement levels (e.g., 0.25-0.75% fiber volume percentage), ii) develop pertinent plastic hinge length expressions accounting for varying axial load levels in order to model UHPC structural responses, and iii) perform benchmark column tests to directly verify numerical modeling tools.

6. Acknowledgements

This material is based upon work supported by the National Science Foundation under Grant No. 2141955. Any opinions, findings, conclusions, or recommendations expressed in this material are those of the author(s) and do not necessarily reflect the views of the National Science Foundation.

7. References

Aboukifa, M., & Moustafa, M. A. (2021). Experimental seismic behavior of ultra-high performance concrete columns with high strength steel reinforcement. *Engineering Structures*, *232*. https://doi.org/10.1016/j.engstruct.2021.111885

Alkaysi, M., & El-Tawil, S. (2016). Effects of variations in the mix constituents of ultra high performance concrete (UHPC) on cost and performance. *Materials and Structures/Materiaux et Constructions*, *49*(10), 4185–4200. https://doi.org/10.1617/s11527-015-0780-6

Applied Technology Council. (2017). *Guidelines for Nonlinear Structural Analysis for Design of Buildings*. https://doi.org/10.6028/NIST.GCR.17-917-46v1

Bae, S., & Bayrak, O. (2008). Seismic Performance of Full-Scale Reinforced Concrete Columns. *ACI Structural Journal*, *105*(2). https://doi.org/10.14359/19727

Bandelt, M. J., & Billington, S. L. (2018). Simulation of Deformation Capacity in Reinforced High-Performance Fiber-Reinforced Cementitious Composite Flexural Members. *Journal of Structural Engineering*, *144*(10), 04018188. https://doi.org/10.1061/(asce)st.1943-541x.0002174

Gencturk, B. (2013). Life-cycle cost assessment of RC and ECC frames using structural optimization. *Earthquake Engineering and Structural Dynamics*, *42*(1), 61–79. https://doi.org/10.1002/eqe.2193

Moreno, D. M., Trono, W., Jen, G., Ostertag, C., & Billington, S. L. (2014). Tension stiffening in reinforced high performance fiber reinforced cement-based composites. *Cement and Concrete Composites*, *50*, 36–46. https://doi.org/10.1016/j.cemconcomp.2014.03.004

Naeimi, N., & Moustafa, M. A. (2021). Compressive behavior and stress–strain relationships of confined and unconfined UHPC. *Construction and Building Materials*, *272*. https://doi.org/10.1016/j.conbuildmat.2020.121844

Paulay, T., & Priestley, M. J. N. (1992). *Seismic Design of Reinforced Concrete and Masonry Buildings*. John Wiley & Sons, Inc.

Pokhrel, M., & Bandelt, M. J. (2019). Plastic hinge behavior and rotation capacity in reinforced ductile concrete flexural members. *Engineering Structures*, *200*. https://doi.org/10.1016/j.engstruct.2019.109699

Russell, H. G., & Graybeal, B. A. (2013). *Ultra-High Performance Concrete: A State-of-the-Art Report for the Bridge Community*. https://www.fhwa.dot.gov/publications/research/infrastructure/structures/hpc/13060/13060.pdf

Shao, Y., & Billington, S. L. (2022). Impact of UHPC Tensile Behavior on Steel Reinforced UHPC Flexural Behavior. *Journal of Structural Engineering*, *148*(1). https://doi.org/10.1061/(asce)st.1943-541x.0003225

Shao, Y., Hung, C.-C., & Billington, S. L. (2021). Gradual Crushing of Steel Reinforced HPFRCC Beams: Experiments and Simulations. *Journal of Structural Engineering*, *147*(8), 04021114. https://doi.org/10.1061/(ASCE)ST.1943-541X.0003080

Shao, Y., & Ostertag, C. P. (2022). Bond-slip behavior of steel reinforced UHPC under flexure: Experiment and prediction. *Cement and Concrete Composites*, *133*. https://doi.org/10.1016/j.cemconcomp.2022.104724

Tariq, H., Jampole, E. A., & Bandelt, M. J. (2021). Development and Application of Spring Hinge Models to Simulate Reinforced Ductile Concrete Structural Components under Cyclic Loading. *Journal of Structural Engineering*, *147*(2). https://doi.org/10.1061/(asce)st.1943-541x.0002891

Wille, K., & Boisvert-Cotulio, C. (2013). *Development of Non-Proprietary Ultra-High Performance Concrete for Use in the Highway Bridge Sector*.

Wille, K., El-Tawil, S., & Naaman, A. E. (2014). Properties of strain hardening ultra high performance fiber reinforced concrete (UHP-FRC) under direct tensile loading. *Cement and Concrete Composites*, *48*, 53–66. https://doi.org/10.1016/j.cemconcomp.2013.12.015